NEOPLASIA
www.neoplasia.com

Volume 10 Number 4 April 2008 pp. 399–407 399

Inhibiting Colorectal Carcinoma Growth and Metastasis By Blocking the Expression of VEGF Using RNA Interference

Shaochuang Wang*[,1], Hui Liu[†,1], Lifeng Ren[‡] Yifeng Pan[‡], and Yangde Zhang*

*National Hepatobiliary and Enteric Surgery Research Center, Ministry of Health, Central South University, Hunan Province, 410008, People's Republic of China; [†]Eastern Hepatobiliary Surgery Hospital, Second Military Medical University, Shanghai 200438, People's Republic of China; [‡]Institute of Biomedical Engineering, Central South University, Xiangya Road, Kai-Fu District, Changsha, Hunan 410008, People's Republic of China

Abstract

Angiogenesis plays an essential role in tumor growth and metastasis and is a promising target for cancer therapy. Vascular endothelial growth factor (VEGF) is a key regulator of angiogenesis. The present study was designed to determine the role of VEGF in tumor growth and metastasis using RNA interference (RNAi) technology. Four small interfering RNA (siRNA) sequences for the VEGF gene were cloned into expression plasmids and transfected into human colorectal carcinoma (CRC) SW620 cells. Stable transfection of these plasmids decreased VEGF protein expression, leading to the potent suppression of tumor cell proliferation, migration, invasion, and angiogenesis *in vitro*. Furthermore, in subcutaneous and intrasplenic/portal injection models involving athymic nude mice, the tumor growth and metastasis of SW620 cells expressing VEGF siRNA were significantly inhibited compared with untransfected cells or cells transfected with control vector alone. Immunohistochemical analyses of tumor sections revealed a decreased vessel density and decreased VEGF expression in the animals where siRNA against VEGF were expressed. These results indicate that RNAi of VEGF can be an effective antiangiogenic strategy for CRC.

Neoplasia (2008) 10, 399–407

Introduction

Colorectal carcinoma (CRC) is the third leading cause of cancer in both men and women and accounts for about 10% of all new cancer cases and cancer deaths in the US [1]. Whereas the overall 5-year survival rate for patients with CRC is 64%, the rate drops to 10% or less in patients with metastatic disease [1]. By the time of diagnosis, 19% of CRC cases are metastatic.

Angiogenesis is an important step in the outgrowth of a primary tumor and a key source for hematogenous tumor dissemination, progression, and metastasis. Many potential angiogenic factors have been characterized, including vascular endothelial growth factor (VEGF) and platelet-derived endothelial cell growth factor [2,3]. VEGF is perhaps the most prominent factor, and it has been extensively studied for its role in the invasion and metastasis of cancer cells. For instance, *in situ* hybridization studies have demonstrated that VEGF mRNA is expressed in the majority of human cancers [4–12].

RNA interference (RNAi) is the sequence-specific, posttranscriptional gene-silencing method initiated by double-stranded RNA that are homologous to the gene being suppressed. Double-stranded RNA are processed by Dicer, a cellular RNase III, to generate duplexes of ~21 nt with 3′-overhangs [small interfering RNA (siRNA)], which mediate sequence-specific mRNA degradation [13,14]. RNAi

Abbreviations: CRC, colorectal carcinoma; ECM, extracellular matrix; Fn, fibronectin; IOD, integrated optical density; MVD, microvascular density; RNAi, RNA interference; siRNA, small interfering RNA; VEGF, vascular endothelial growth factor; VEGFR, VEGF receptor

[1]These authors contributed equally to this work.

Address all correspondence to: Yangde Zhang, Xiangya Road, Kai-Fu District, Changsha, Hunan, China. E-mail: zyd@2118.cn

Received 17 July 2007; Revised 22 October 2007; Accepted 25 October 2007

DOI 10.1593/neo.07613

technology, especially chemically synthesized siRNA, is currently being evaluated not only as a powerful tool for functional genomic analyses but also as a potentially useful method to develop highly specific gene-silencing therapeutics. Previous studies have shown that inhibition of VEGF by siRNA decreases tumor growth in several animal models [15,16].

The high efficiency and specificity of RNA-mediated interference has made it a powerful and widely used tool for the analysis of gene function. In this report, we used a vector-based VEGF siRNA expression system to suppress the expression of VEGF in SW620 human CRC cells and to evaluate its therapeutic efficacy in a xenograft model. The vector-based RNAi technology may overcome the limitations of transience and high cost associated with synthetic siRNA and, more importantly, it may make *in vivo* testing possible.

Materials and Methods

Cell Culture

ECV304 cells and the CRC cell line SW620 (Laboratory of Cell Biology, Xiangya Medical School, Changsha, China) were maintained in RPMI 1640 medium containing 10% fetal bovine serum, 100 μg/ml penicillin, and 100 μg/ml streptomycin. Routine testing confirmed that the cells were free of *Mycoplasma* and viral contaminants during the entire study period.

Generation of VEGF siRNA Expression Plasmids

We selected siRNA sequences as reported by Elbashir et al. [17]. We used the following procedure to design the VEGF siRNA: 1) search for the sequences 5′-AA(N19) or 5′-NA(N19), where N is any nucleotide, in the intended mRNA sequence, and use only those sequences that occur within an open reading frame, preferably 50 to 100 nt downstream of the start codon, and show 47% or 52% G/C content; 2) perform a BLAST search with the selected siRNA sequences against expressed sequence tag libraries to ensure that only a single gene is targeted; and 3) search for any predicted secondary structure of the target mRNA that might inhibit siRNA binding. Four siRNA targeting human VEGF and one scrambled siRNA (used for a negative control) with the following sense and antisense sequences were used: VEGF siRNA no. 1, 5′-GGCGTCGCACTGAAACTTT-3′ (sense) and 5′-AAAGTTTCAGTGCGACGCC-3′ (antisense); VEGF siRNA no. 2, 5′-ACCTCACCAAGGCCAGCAC-3′ (sense) and 5′-GTGCT GGCC TTGG T GAG GT-3′ (antisense); VEGF siRNA no. 3, 5′-GGG CAGAA TCA TCA C GAAG-3′ (sense) and 5′-CTTCGTGATGATTCTGCCC-3′ (antisense); VEGF siRNA no. 4, 5′-GGCCAGCACATAGGAGAGA-3′ (sense) and 5′-TCTCTCCTATGTG CTGGCC-3′ (antisense); and negative VEGF siRNA control, 5′-GACTTCATAAGGCGCATGC-3′ (sense) and 5′-GC ATGCGCCTTATGAAGTC-3′ (antisense). All siRNA were designed and synthesized by Wuhan Genesil Biotechnology Co., Ltd., Wuhan, China. Sense and antisense primers containing the sense siRNA sequence, 9 bp loop sequence, antisense siRNA sequence, and RNA polymerase III terminator sequence were created with *Bam*HI and *Hin*dIII restriction sites on the 5′ and 3′ ends, respectively. These primers were annealed and inserted into pGenesil-1 (Wuhan Genesil Biotechnology Co, Ltd.) downstream of the H1 RNA polymerase III promoter, following the manufacturer's instructions. The resultant plasmids containing siRNA sequences 1, 2, 3, and 4 and negative control sequences were named pSihVEGF-1, pSihVEGF-2, pSihVEGF-3, pSihVEGF-4, and pHK, respectively.

Stable Transfection of siRNA

SW620 cells were stably transfected with pSihVEGF-1, pSihVEGF-2, pSihVEGF-3, pSihVEGF-4, or pHK in the presence of Lipofectamine 2000 (Invitrogen, Guangzhou, China) following the manufacturer's instructions and placed under G418 selection for 4 weeks. Surviving colonies were isolated and expanded. Surviving colonies containing pSihVEGF-1, pSihVEGF-2, pSihVEGF-3, pSihVEGF-4, or pHK were named SihVEGF-1, SihVEGF-2, SihVEGF-3, SihVEGF-4, or HK, respectively.

VEGF ELISA and Western Blot Analysis

The secretion of VEGF by stably transfected cells was determined using a Quantikine human VEGF Immunoassay kit (R&D Systems, Minneapolis, MN) according to the manufacturer's instructions. All the experiments were done in triplicate.

For analysis of intracellular VEGF protein levels, untransfected and transfected SW620 cells were cultured in 100-mm dishes and when cells reached 80% confluence, cell lysates were collected and protein concentrations determined using the BCA Protein Assay Reagent Kit (Pierce Corporation, Rockford, IL). The protein samples (50 μg) were boiled for 3 minutes before being loaded onto a 7.5% SDS–polyacrylamide gel and, after electrophoresis, the proteins were transferred to a nitrocellulose membrane (Amersham, Piscataway, NJ). The membranes were probed with primary antibody followed by peroxidase-conjugated secondary antibody and visualized by the enhanced chemiluminescene detection system (Amersham) according to the manufacturer's instructions.

MTT Assay

Cell proliferation was measured by the MTT assay. SW620, SihVEGF-4, and HK cells were seeded in 24-well plates at a density of 1×10^4 cells/well. After a 24-hour incubation, 200 μl of 5 mg/μl solution of MTT (Sigma, Guangzhou, China) in PBS was added to each well. The plates were then incubated for 4 hours at 37°C. The precipitate was then solubilized in 100% dimethylsulfoxide (Sigma), 100 μl/well, and shaken for 15 minutes. Absorbance of each well was measured on a microplate reader (Wellwash MK2; Labsystems Dradon, Helsinki, Finland) at a wavelength of 492 nm. All experiments were done in quadruplicate.

Flow Cytometry

Flow cytometry was used to further assess the mechanisms responsible for the decreased proliferation seen in SW620, SihVEGF-4, and HK cells. The harvested cells were washed with PBS, fixed with 70% ethanol, treated with RNase A (Sigma) and then stained with propidium iodide (Sigma). Finally, cell cycle analysis was carried out using a flow cytometer.

Adhesion Assay

The SW620, SihVEGF-4, and HK cells were seeded in quadruplicate at a density of 1×10^4 cells/well in 96-well plates coated with BSA (10 g/l), Matrigel (50 mg/l), or fibronectin (Fn) (10 mg/l). The cells were cultured at 37°C for 60 minutes, and the MTT assay was performed as above.

Tumor Cell Adherence to ECV304

ECV304 cells were plated onto 96-well plates at a density of 5×10^4 cells/well. After 48 hours, the supernatant was aspirated and SW620, SihVEGF-4, and HK cells were plated at a density of 5×10^4 cells/well. After 30 minutes, the wells were gently washed twice with PBS to remove unattached cells, and 100 μl of rose bengal (25%) was added for 5 minutes. The supernatant was aspirated, the wells were gently washed twice with PBS, and finally 200 μl 95% ethanol/PBS (1:1) was added. After 20 minutes, the absorbance at 570 nm was recorded.

Migration Assay

The SW620, SihVEGF-4, and HK cells were plated onto 12-well plates at a density of 8×10^4 cells/well. After forming monolayers, cells were wounded by manual scraping with a 200-micropipette tip. The culture medium was then replaced with fresh, serum-free medium. Wound closure was monitored at various time points by observation under a microscope and the degree of cell migration was quantified by the ratio of gap distance at 24 hours to that at 0 hour. The experiment was done in triplicate.

Invasion Assay

The invasion assays with SW620, SihVEGF-4, and HK cells were performed using Transwell polycarbonate membrane inserts in 24-well plates (Corning, Lowell, MA) following the manufacturer's instructions. Briefly, the underside of each polycarbonate microporous membrane was coated with Matrigel (1:100) at 37°C for 5 minutes and allowed to sit overnight. Then, 50 μl Matrigel (1:30) and 200 μl sterile water were added to the upper compartment at 37°C. After 2 days, 200 μl of the invasion buffer [2 ml BSA (2%) + 38 ml RPMI 1640] was added into the upper compartment and, 1 hour later, the upper compartment fluid was aspirated. SW620, SihVEGF-4, or HK cells at a density of 5×10^4 cells/well were added into the upper compartment, and 800 μl of the Fn solution (10 μg/ml) was added into the lower compartment. The cells were allowed to migrate for 48 hours. The inserts were then fixed in 10% formalin, stained with hematoxylin and eosin, and rinsed by dipping in water. The cells on the upper surface of the membrane were removed with a cotton bud. The membranes were air-dried overnight, excised from the insert, and mounted onto glass slides for microscopic analysis. The migrated cells were counted at high-power magnification (×40) from four randomly selected fields. Each experiment was repeated three times.

In Vitro *Angiogenesis Assay*

The test was performed using the *In vitro* Angiogenesis Assay Kit (Chemicon International, Temecula, CA) following the manufacturer's instructions. Briefly, 96-well plates were coated with cold solution (50 μl/well of a solution containing 900 μl of ECMatrix per 100 μl of 10× diluent buffer), which was allowed to polymerize at room temperature for about 60 minutes. Then, wells were seeded with 100 μl of a 5×10^4 cells/ml suspension of ECV304, ECV304 transiently transfected with pHK, or ECV304 transiently transfected with pSihVEGF-4. Tube formation was assessed after 12 hours.

Murine Xenograft Model

Male BALB/c athymic nude mice, 4 to 6 weeks old, were injected subcutaneously with 2×10^6 SW620, SihVEGF-4, or HK cells. Tumor diameters were measured at regular intervals with digital calipers, and the tumor volume in mm^3 was calculated by the formula: volume = $(\text{width})^2 \times \text{length}/2$ [18]. Every group had three mice. Animal experiments in the present study were performed in compliance with the guidelines of the Institute for Xiangya Medical School, Central South University.

Experimental liver metastases were generated by intrasplenic/portal injection of tumor cells (SW620, SihVEGF-4, or HK cells) as described previously [19]. The mice were inoculated with 2×10^6 cells and splenectomized 1 minute later. Every group had three mice. Animals were killed 5 weeks later, and liver metastases were counted immediately without prior fixation.

Immunohistochemical Analysis

Immunohistochemical staining for CD31 and microvessel counting of CD31-positive vessels were performed as described previously [20]. Immunohistochemical determination of VEGF was also performed as described previously [21].

Statistical Analysis

All results are expressed as means ± SD. Statistical analyses were performed using the Statistical Package for the Social Sciences (SPSS Inc., Chicago, IL), and statistical significance was set at $P < .05$.

Results

Effects of VEGF siRNA on the Expression of VEGF

Four VEGF siRNA–expressing plasmids (plasmids 1, 2, 3, and 4) and one negative control plasmid (pHK) were constructed using the pGenesil-1 vector. The pGenesil-1 vector encodes enhanced green fluorescence protein, so that if the VEGF siRNA–expressing plasmids are successfully transfected into the SW620 cells, they can be detected by fluorescence microscopy. As shown in Figure 1, the transfections were successful, and five stably transfected cell lines could be constructed. The VEGF protein levels were measured by ELISA and Western blot analysis. As shown in Figure 2*A*, VEGF siRNA significantly inhibited VEGF expression in four cell lines as measured by ELISA: SihVEGF-1 (74.75% of expression in untransfected cells), SihVEGF-2 (61.72%), SihVEGF-3 (69.21%), and SihVEGF-4 (97.46%). The inhibition reached statistical significance ($P < .001$), whereas the slight inhibition observed in HK cells (2.04%) ($P > .05$). Western blot analysis confirmed the inhibition of VEGF expression by the four VEGF siRNA constructs (Figure 2*B*). Subsequent experiments focused on the VEGF siRNA no. 4 because it was the most effective at inhibiting VEGF expression.

Effects of VEGF siRNA on Tumor Cell Proliferation

The biological effects of the VEGF siRNA were first determined using cell proliferation assays. As shown in Figure 3 SihVEGF-4 cell proliferation was significantly inhibited at days 3 and 4 ($P < .001$, compared with the controls), whereas there was little difference between the negative control cells (HK) and untransfected SW620 cells over the entire experimental period ($P > .05$). The VEGF siRNA were also found to have an effect on the cell cycle (Figure 4): 67.0% of SihVEGF-4 cells were in the G_1 phase, which was significantly higher than the fraction for HK cells (54.5%) or untransfected SW620

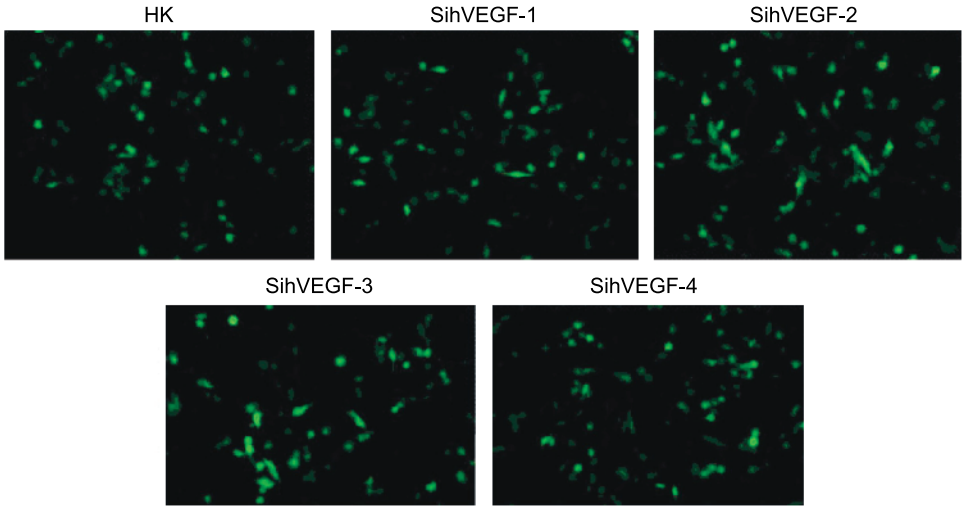

Figure 1. Transfection of VEGF siRNA into cells. The pGenesil-1 vector was used to construct plasmids expressing VEGF siRNA and EGFP as a fluorescence probe. Stably transfected SW620 cells (SihVEGF-1, SihVEGF-2, SihVEGF-3, SihVEGF-4, and HK control cells) could be easily identified by fluorescence microscopy.

cells (50.8%), suggesting that the VEGF siRNA arrests cells in the G_1 phase.

Effects of the VEGF siRNA on Tumor Cell Adhesion

Suppressing VEGF expression had a clear inhibitory effect on the adhesion of transfected colon cancer cells to the extracellular matrix (ECM) [Matrigel and Fn] and to ECV304. The percentages of adhesion to ECM were as follows: SW620, 36.23% (Fn) and 86.42% (Matrigel); HK, 38.84% (Fn) and 84.77% (Matrigel); and SihVEGF-4, 9.13% (Fn) and 41.2% (Matrigel) (Figure 5*A*). The tumor cell lines showed different absorbance abilities: SW620, 0.611; HK, 0.585; and SihVEGF-4, 0.283 (Figure 5*B*). Thus, the adhesion of SihVEGF-4 to ECM and to ECV304 cells was significantly suppressed ($P < .001$), whereas there was little difference between untransfected cells and negative control HK cells ($P > .05$).

Effects of VEGF siRNA on Tumor Cell Migration

As shown in Figure 6, the migration distance of untransfected SW620, HK, and SihVEGF-4 was 1.8, 1.75, and 0.83 mm, respectively. These findings suggest that the migration of SihVEGF-4 was significantly suppressed ($P < .001$), whereas there was little difference between untransfected cells and the negative control (HK) ($P > .05$).

Effects of VEGF siRNA on Tumor Cell Invasion

As shown in Figure 7*A*, for each 400× field under the microscope, the number of migrated SihVEGF-4 cells was 246 ± 23, significantly

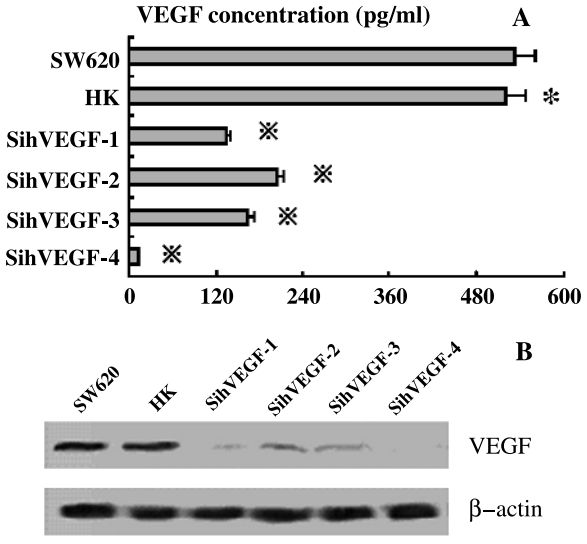

Figure 2. Effects of VEGF siRNA on VEGF expression in transfected cells. (A) ELISA was used to measure the amount of VEGF in supernatants from SihVEGF-1, SihVEGF-2, SihVEGF-3, SihVEGF-4, HK, and untransfected SW620 cells. *$P > .05$, ※ $P < .001$. (B) Western blot analysis was used to measure the amount of VEGF in SihVEGF-1, SihVEGF-2, SihVEGF-3, SihVEGF-4, HK, and untransfected SW620 cells.

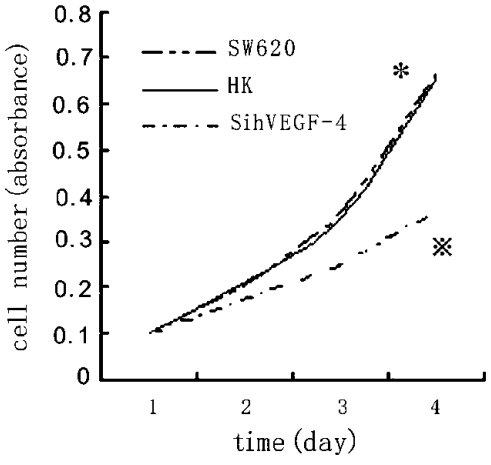

Figure 3. Effects of VEGF siRNA on tumor cell proliferation as measured by the MTT assay. *$P > .05$, ※ $P < .001$.

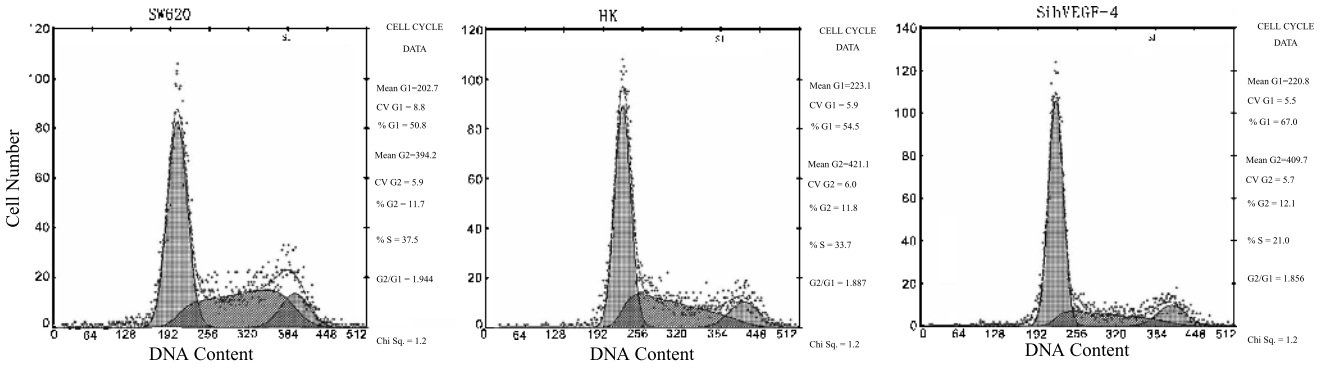

Figure 4. Effects of VEGF siRNA on tumor cell cycle distribution.

lower than the number of untransfected cells (446 ± 15) and the negative control HK cells (438 ± 14) ($P < .001$). In addition, there was little difference between untransfected cells and the negative control (HK) ($P > .05$).

Effects of VEGF siRNA on Angiogenesis In Vitro

As shown in Figure 7*B*, *in vitro* tube formation of ECV304 cells transiently transfected with pSihVEGF-4 was 35 ± 4 per 100× field, which was significantly lower ($P < .001$) compared with untransfected ECV304 (117 ± 9) and ECV304 transiently transfected with pHK (121 ± 5). Moreover, there was little difference between untransfected ECV304 and ECV304 transiently transfected with pHK ($P > .05$).

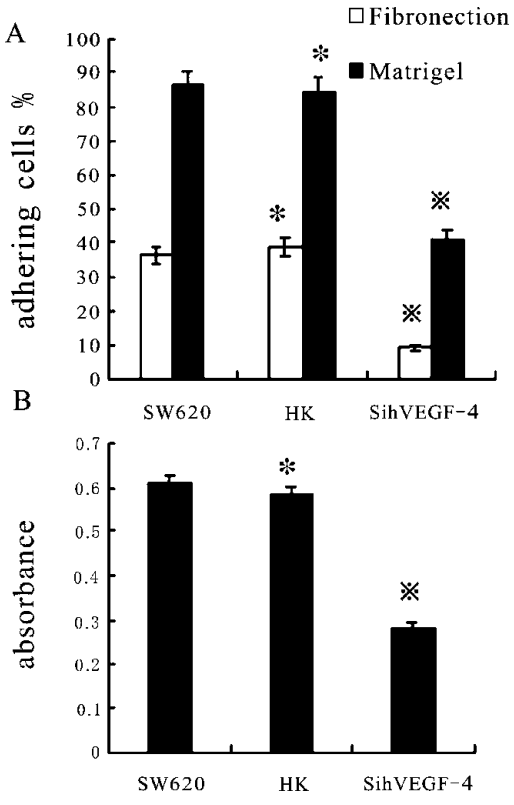

Figure 5. Effects of VEGF siRNA on tumor cell adhesion. (A) Tumor cell adhesion to ECM (Fn and Matrigel). *$P > .05$, ※ $P < .001$. (B) Tumor cell adhesion to ECV304. *$P > .05$, ※ $P < .001$.

Effects of VEGF siRNA on CRC Tumor Growth and Metastasis In Vivo

As shown in Figure 8, SW620 and HK cells grew rapidly. In contrast, tumor formation was significantly delayed in the case of SihVEGF-4.

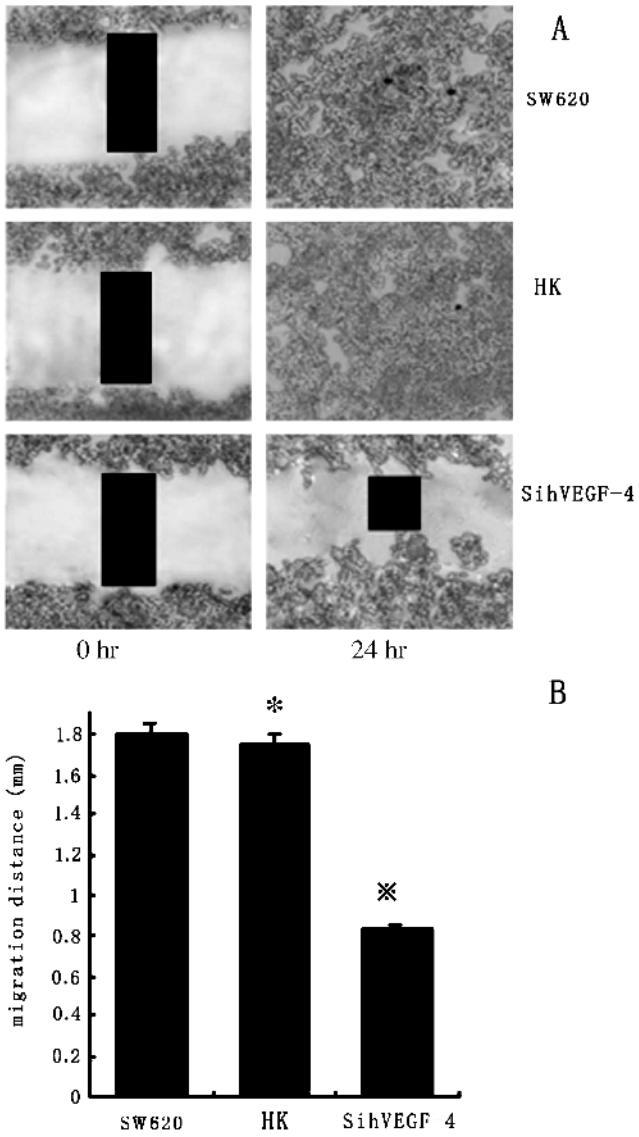

Figure 6. Effects of VEGF siRNA on tumor cell migration. *$P > .05$, ※ $P < .001$.

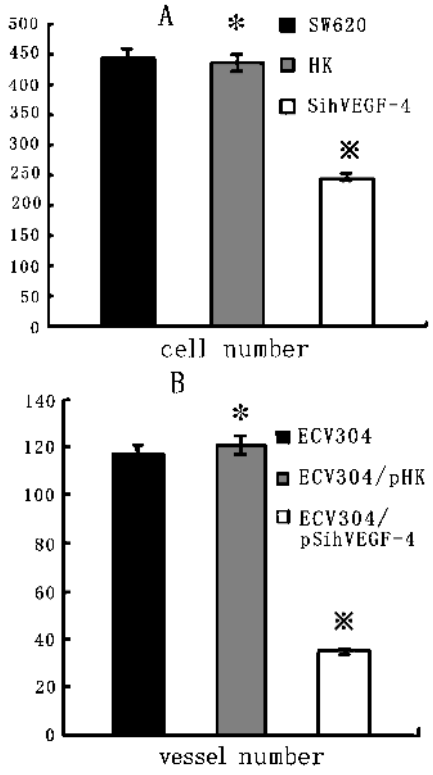

Figure 7. Effects of VEGF siRNA on tumor cell invasion and angiogenesis *in vitro*. (A) Tumor cell invasion. *$P > .05$, ※ $P < .001$. (B) Angiogenesis *in vitro*. *$P > .05$, ※ $P < .001$.

In addition, the SihVEGF-4 tumors were significantly smaller than those in untransfected SW620 cells and in the HK negative control ($P < .001$).

In a model of CRC liver metastasis, the untransfected SW620 and HK groups showed an increased number of metastatic tumors compared to the SihVEGF-4 group, and their body weight decreased significantly after 28 days (Figure 9). In contrast, metastatic tumors in the SihVEGF-4 group formed in only one nude mouse ($n = 3$) and the body weight of nude mice decreased slowly from 28 days.

Immunohistochemical Findings

Tumor tissue from mice was excised and subjected to immunohistochemical staining. As shown in Figure 10, the microvascular density (MVD) values (per 200× field) of subcutaneous tumors in SW620, HK, and SihVEGF-4 cell lines were 14 ± 2, 12 ± 1, and 4 ± 1, respectively. The MVD values of liver metastatic tumors in SW620, HK, and SihVEGF-4 cell lines were 17 ± 2, 15 ± 3, and 7 ± 2, respectively. These results indicate that CD31-positive vessels were abundant in subcutaneous tumors and liver metastatic tumors in the SW620 and HK lines ($P > .05$), whereas vessel density in both tumor types was significantly decreased in the SihVEGF-4 group ($P < .001$).

VEGF staining was much higher in subcutaneous tumor and liver metastatic tumors of SW620 and negative control cells (Figure 11). In contrast, VEGF staining was significantly decreased in both tumor types for the SihVEGF-4 group. Quantitative data for VEGF immunohistochemical staining was analyzed using Image Pro Plus 6.0 (Media Cybernetics, Shanghai, China). The integrated optical density (IOD) values of subcutaneous tumors of SW620, HK, and SihVEGF-4 cells were 1900.75 ± 84.09, 1984.93 ± 5.36, and 1274.25 ± 57.16, respectively (Figure 12). For liver metastatic tumors, the corresponding IOD values were 2115.96 ± 107.93, 2103.45 ± 31.17, and 575.97 ± 13.76, respectively. As shown in Figures 11 and 12, VEGF staining was much higher in subcutaneous tumor and liver metastasis tumors of SW620 and negative group (HK) ($P > .05$). In contrast, VEGF staining was significantly decreased in SihVEGF-4 group both in subcutaneous and liver metastasis tumors ($P < .001$).

Discussion

VEGF is one of the most important angiogenic factors. Its role in angiogenesis and tumor development, growth, and metastasis has been well documented [15,16]. When secreted by tumor cells, it acts in a paracrine fashion to stimulate proliferation of endothelial cells [22]. Although endothelial cells are the primary targets of

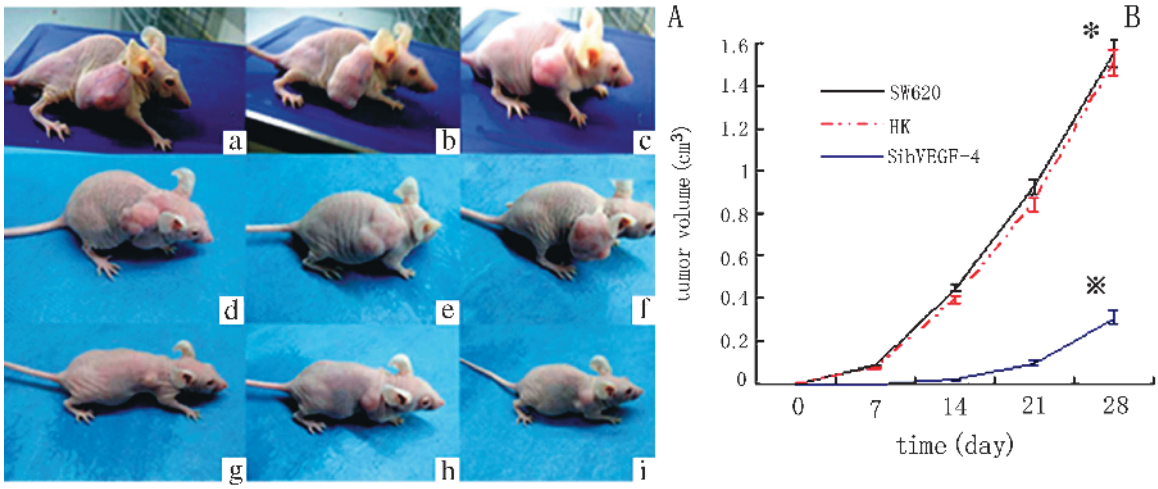

Figure 8. Effects of VEGF siRNA on tumor growth *in vivo*. (A) Subcutaneous tumor model: SW620 group (a, b, c; $n = 3$), HK group (d, e, f; $n = 3$), and SihVEGF-4 group (g, h, i; $n = 3$). (B) Tumor growth curves of each group over 28 days. *$P > .05$, ※ $P < .001$.

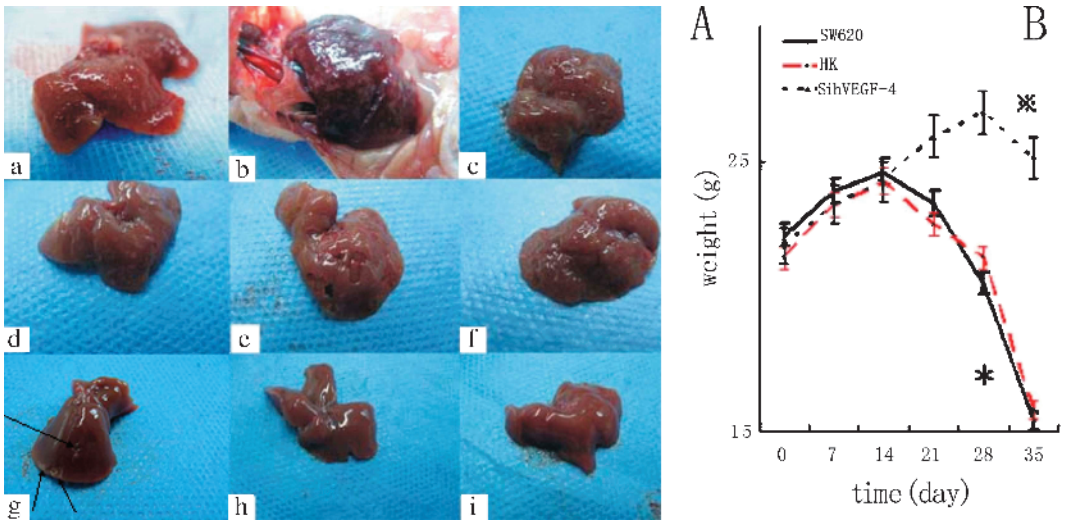

Figure 9. Effects of VEGF siRNA on tumor metastasis *in vivo*. (A) Liver metastasis model: SW620 group (a, b, c; $n = 3$), HK group (d, e, f; $n = 3$), and SihVEGF-4 group (g, h, i; $n = 3$). Arrow shows metastasis in SihVEGF-4 group (1/3). (B) Body weight change in SW620 group, HK group, and SihVEGF-4 group over 35 days. *$P > .05$, ※ $P < .05$.

VEGF, several studies have also reported its mitogenic effects on certain nonendothelial cells, such as retinal pigment epithelial cells [23], pancreatic duct cells [24], and Schwann cells [25]; as well as on cancer cells, including breast cancer [26–28], prostate cancer [29,30], and gastric adenocarcinoma [31]. These findings have led us to hypothesize that an autocrine loop exists whereby VEGF stimulates tumor growth not only by interacting with endothelial cells but also by binding directly to the VEGF receptor (VEGFR) on tumor cells.

The present study demonstrated that RNA interference against VEGF successfully inhibited the expression and secretion of VEGF in human CRC SW620 cells, leading to a potent suppression of tumor cell proliferation, migration, invasion, angiogenesis *in vitro* and *in vivo*, as well as tumor growth, and metastasis in a xenograft tumor model. These findings not only demonstrate that VEGF plays a critical role in colon cancer cell proliferation, migration, and invasion but also suggest that a VEGF-mediated autocrine loop is a significant factor affecting tumor growth and metastasis.

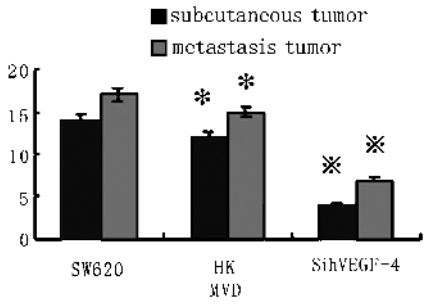

Figure 10. Effects of VEGF siRNA on tumor angiogenesis *in vivo*. The MVD values (per 200× field) of subcutaneous and metastatic tumors are as follows: SW620 group: 14 ± 2 (subcutaneous) *vs* 17 ± 2 (metastatic tumor); HK group: 12 ± 1 (subcutaneous) *vs* 15 ± 3 (metastasis); SihVEGF-4 group: 4 ± 1 (subcutaneous) *vs* 7 ± 2 (metastatic). *$P > .05$, ※ $P < .001$.

Recent reports by Detwiller et al. [15] and Guan et al. [16] demonstrate that siRNA-targeting VEGF decrease sarcoma growth *in vivo* but have no effect on cellular proliferation *in vitro*. In the present study, we have found that the VEGF siRNA suppresses not only the proliferation of SW620 cells but also their ability to migrate and invade. The effects on proliferation, migration, and invasion appear to be a direct effect of the decreased production of VEGF by these cells. Our findings and previous studies [32,33] support the idea that there may be a VEGF-directed autocrine loop directly affecting colon cancer cell growth and function. Studies suggest that mechanisms of VEGF/VEGFR interaction may involve the cyclooxygenase-2 inhibitor and activation of the Src family [32,33], but the specific mechanisms of VEGF/VEGFR interaction in both endothelial and tumor cells remain unclear. More research is needed to delineate the signaling pathways mediated by VEGFRs.

Even with a nearly complete abrogation of VEGF protein secretion, SW620 cells still formed tumors in mice, albeit at a significantly slower rate. This indicates that there may be several additional mechanisms involved in angiogenesis that is stimulated in VEGF-silenced tumors. For instance, tumors may induce surrounding stromal cells to secrete VEGF. It has been shown in tumors derived from VEGF-null embryonic stem cells that VEGF-A from tumor stroma can support tumor vascularization [33]. Perhaps RNAi targeting multiple angiogenic factors could completely abrogate new blood vessel formation and tumor growth.

In considering RNAi as a therapeutic tool, one must consider methods of delivery, because the efficacy and mode of delivery of siRNA vary considerably [34]. Chemically or enzymatically synthesized siRNA is costly and has been shown to have a relatively short half-life, with only transient inhibition of target genes [35]. These and other problems have been addressed through changes in how the RNAi is delivered. For example, repeated administration of siRNA can compensate for the reagent's short half-life. In addition, the use of ligand-directed nanoparticles has shown promise in addressing other RNAi issues, such as cellular uptake, nonspecific immune stimulation, and limited stability [36]. The present study corroborates other

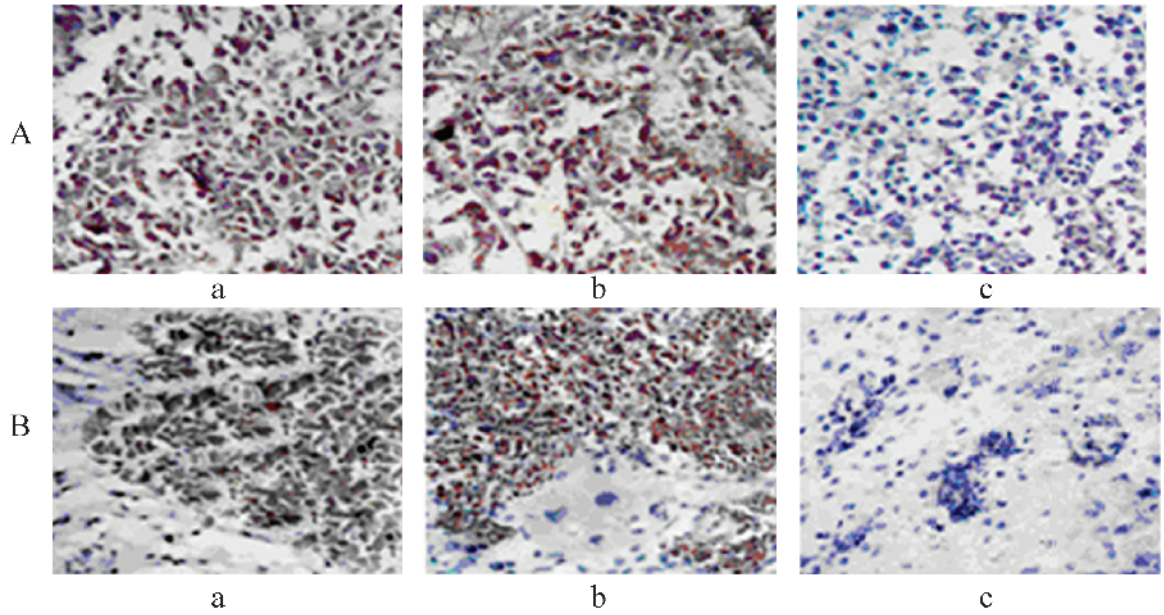

Figure 11. Effects of VEGF siRNA on VEGF expression *in vivo* as determined by immunohistochemistry. (A) VEGF expression in subcutaneous tumors: SW620 group (a), HK group (b), SihVEGF-4 group (c). (B) VEGF expression in metastatic tumors: SW620 group (a), HK group (b), and SihVEGF-4 group (c).

work [37,38] to highlight another technique: the use of plasmid and viral vectors to produce siRNA using the polymerase III promoter. This approach may offer more efficient siRNA delivery and can theoretically induce stable gene silencing.

In summary, the present study demonstrated that vector-mediated RNA interference of VEGF successfully inhibited the expression of VEGF in *in vitro* and *in vivo* models of human CRC, leading to several antitumor activities such as inhibitory effects on cell proliferation, migration, invasion, angiogenesis, tumor growth, and metastasis. These findings suggest that the RNAi approach can be an effective therapeutic strategy for CRC. The present study provides a basis for future studies of this approach in additional animal models and in human clinical trials.

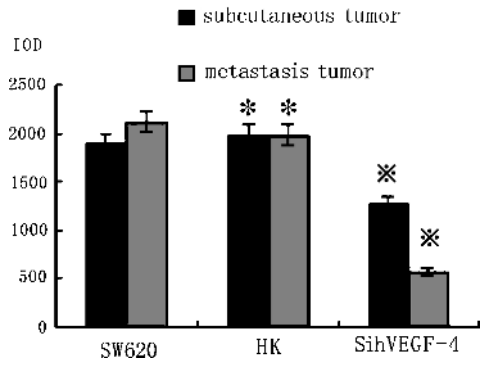

Figure 12. Quantitative data for VEGF immunohistochemical staining. IOD values of VEGF expression were determined using Image Pro Plus 6.0. SW620 group: 1900.75 ± 84.09 (subcutaneous) *vs* 2115.96 ± 107.93 (metastatic); HK group: 1984.93 ± 5.36 (subcutaneous) *vs* 2103.45 ± 31.17 (metastatic); SihVEGF-4 group 1274.25 ± 57.16 (subcutaneous) *vs* 575.97 ± 13.76 (metastatic). *$P > .05$, ※$P < .001$.

Acknowledgments

We thank Cheng Huan and Zhiyong Luo for helpful discussions and for critical reading of the manuscript, and we are grateful to our colleagues in the Laboratory of Cell Biology, Xiangya Medical School, Central South University, for their excellent technical support.

References

[1] Jemal A, Siegel R, Ward E, Murray T, Xu J, and Thun J (2007). Cancer statistics, 2007. *CA Cancer J Clin* **57**, 43–66.

[2] Leung DW, Cachianes G, Kuang WJ, Goeddel DV, and Ferrara N (1989). Vascular endothelial growth factor is a secreted angiogenic mitogen. *Science* **246**, 1306–1309.

[3] Takahashi Y, Bucana CD, Liu W, Yoneda J, Kitadai Y, Cleary KR, and Ellis LM (1996). Platelet-derived endothelial cell growth factor in human colon cancer angiogenesis: role of infiltrating cells. *J Natl Cancer Inst* **88**, 1146–1151.

[4] Volm M, Koomägi R, Mattern J, and Stammler G (1997). Angiogenic growth factors and their receptors in non–small cell lung carcinomas and their relationships to drug response *in vitro*. *Anticancer Res* **17**, 99–103.

[5] Yoshiji H, Gomez DE, Shibuya M, and Thorgeirsson UP (1996). Expression of vascular endothelial growth factor, its receptor, and other angiogenic factors in human breast cancer. *Cancer Res* **56**, 2013–2016.

[6] Ferrara N and Davis-Smyth T (1997). The biology of vascular endothelial growth factor. *Endocr Rev* **18**, 4–25.

[7] Suzuki K, Hayashi N, Miyamoto Y, Yamamoto M, Ohkawa K, Ito Y, Sasaki Y, Yamaguchi Y, Nakase H, Noda K, et al. (1996). Expression of vascular permeability factor/vascular endothelial growth factor in human hepatocellular carcinoma. *Cancer Res* **56**, 3004–3009.

[8] Ellis LM, Takahashi Y, Fenoglio CJ, Cleary KR, Bucana CD, and Evans DB (1998). Vessel counts and vascular endothelial growth factor expression in pancreatic adenocarcinoma. *Eur J Cancer* **34**, 337–340.

[9] Uchida S, Shimada Y, Watanabe G, Tanaka H, Shibagaki I, Miyahara T, Ishigami S, and Imamura M (1998). In oesophageal squamous cell carcinoma vascular endothelial growth factor is associated with p53 mutation, advanced stage and poor prognosis. *Br J Cancer* **77**, 1704–1709.

[10] Tomisawa M, Tokunaga T, Oshika Y, Tsuchida T, Fukushima Y, Sato H, Kijima H, Yamazaki H, Ueyama Y, Tamaoki N, et al. (1999). Expression pattern of vascular endothelial growth factor isoform is closely correlated with tumour stage and vascularisation in renal cell carcinoma. *Eur J Cancer* **35**, 133–137.

[11] Sowter HM, Corps AN, and Evans AL (1997). Expression and localization of the vascular endothelial growth factor family in ovarian epithelial tumors. *Lab Invest* **77**, 607–614.

[12] Guidi AJ, Abu-Jawdeh G, Tognazzi K, Dvorak HF, and Brown LF (1996). Expression of vascular permeability factor (vascular endothelial growth factor) and its receptors in endometrial carcinoma. *Cancer* **78**, 454–460.

[13] Elbashir SM, Harborth J, Lendeckel W, Yalcin A, Weber K, and Tuschl T (2001). Duplexes of 21-nucleotide RNAs mediate interference in cultured mammalian cells. *Nature (Lond)* **411**, 494–498.

[14] Fire A, Xu S, Montgomery MK, Kostas SA, Driver SE, and Mello CC (1998). Potent and specific genetic interference by double-stranded RNA in *Caenorhabditis elegans*. *Nature (Lond)* **391**, 806–811.

[15] Detwiller KY, Fernando NT, Segal NH, Ryeom SW, D'Amore PA, and Yoon SS (2005). Analysis of hypoxia-related gene expression in sarcomas and effect of hypoxia on RNA interference of vascular endothelial cell growth factor A. *Cancer Res* **65**, 5881–5889.

[16] Guan H, Zhou ZC, Wang H, Jia SF, Liu W, and Kleinerman ES (2005). A small interfering RNA targeting vascular endothelial growth factor inhibits Ewing's sarcoma growth in a xenograft mouse model. *Clin Cancer Res* **11**, 2662–2669.

[17] Elbashir SM, Harborth J, Weber K, and Tuschl T (2002). Analysis of gene function in somatic mammalian cells using small interfering RNAs. *Methods* **26**, 199–213.

[18] Burfeind P, Chernicky CL, Rininsland F, and Ilan J (1996). Antisense RNA to the type I insulin–like growth factor receptor suppresses tumor growth and prevents invasion by rat prostate cancer cells *in vivo*. *Proc Natl Acad Sci USA* **93**, 7263–7268.

[19] Long L, Rubin R, and Brodt P (1998). Increased invasive and metastatic potential in tumor cells overexpressing the receptor for type 1 insulin–like growth factor receptor. *Exp Cell Res* **238**, 116–121.

[20] Takei Y, Kadomatsu K, Matsuo S, Itoh H, Nakazawa K, Kubota S, and Muramatsu T (2001). Antisense oligodeoxynucleotide targeted to midkine, a heparin-binding growth factor, suppresses tumorigenicity of mouse rectal carcinoma cells. *Cancer Res* **61**, 8486–8491.

[21] Park YW, Younes MN, Jasser SA, Yigitbasi OG, Zhou G, Bucana CD, Bekele BN, and Myers JN (2005). AEE788, a dual tyrosine kinase receptor inhibitor, induces endothelial cell apoptosis in human cutaneous squamous cell carcinoma xenografts in nude mice. *Clin Cancer Res* **11**, 1963–1973 [March 1].

[22] Ohta Y, Endo Y, Tanaka M, Shimizu J, Oda M, Hayashi Y, Watanabe Y, and Sasaki T (1996). Significance of vascular endothelial growth factor messenger RNA expression in primary lung cancer. *Clin Cancer Res* **2**, 1411–1416.

[23] Guerrin M, Moukadiri H, Chollet P, Moro F, Dutt K, Malecaze F, and Plouët J (1995). Vasculotropin/vascular endothelial growth factor is an autocrine growth factor for human retinal pigment epithelial cells cultured *in vitro*. *J Cell Physiol* **164**, 385–394.

[24] Oberg-Welsh C, Sandler S, Andersson A, and Welsh M (1997). Effects of vascular endothelial growth factor on pancreatic duct cell replication and the insulin production of fetal islet-like cell clusters *in vitro*. *Mol Cell Endocrinol* **126**, 125–132.

[25] Sondell M, Lundborg G, and Kanje M (1999). Vascular endothelial growth factor has neurotrophic activity and stimulates axonal outgrowth, enhancing cell survival and Schwann cell proliferation in the peripheral nervous system. *J Neurosci* **19**, 5731–5740.

[26] Kranz A, Mattfeldt T, and Waltenberger J (1999). Molecular mediators of tumor angiogenesis: enhanced expression and activation of vascular endothelial growth factor receptor KDR in primary breast cancer. *Int J Cancer* **84**, 293–298.

[27] Bachelder RE, Crago A, Chung J, Wendt MA, Shaw LM, Robinson G, and Mercurio AM (2001). Vascular endothelial growth factor is an autocrine survival factor for neuropilin-expressing breast carcinoma cells. *Cancer Res* **61**, 5736–5740.

[28] Nakopoulou L, Stefanaki K, Panayotopoulou E, Giannopoulou I, Athanassiadou P, Gakiopoulou-Givalou H, and Louvrou A (2002). Expression of the vascular endothelial growth factor receptor-2/Flk-1 in breast carcinomas: correlation with proliferation. *Hum Pathol* **33**, 863–870.

[29] Soker S, Kaefer M, Johnson M, Klagsbrun M, Atala A, and Freeman MR (2001). Vascular endothelial growth factor–mediated autocrine stimulation of prostate tumor cells coincides with progression to a malignant phenotype. *Am J Pathol* **159**, 651–659.

[30] Jackson MW, Roberts JS, Heckford SE, Ricciardelli C, Stahl J, Choong C, Horsfall DJ, and Tilley WD (2002). A potential autocrine role for vascular endothelial growth factor in prostate cancer. *Cancer Res* **62**, 854–859.

[31] Tian X, Song SM, Wu J, Meng L, Dong Z, and Shou C (2001). Vascular endothelial growth factor: acting as an autocrine growth factor for human gastric adenocarcinoma cell MGC803. *Biochem Biophys Res Commun* **286**, 505–512.

[32] Kim SJ, Seo JH, Lee YJ, Yoon JH, Choi CW, Kim BS, Shin SW, Kim YH, and Kim JS (2005). Autocrine vascular endothelial growth factor/vascular endothelial growth factor receptor-2 growth pathway represents a cyclooxygenase-independent target for the cyclooxygenase-2 inhibitor NS-398 in colon cancer cells. *Oncology* **68**, 204–211.

[33] Viloria-Petit A, Miquerol L, Yu JL, Gertsenstein M, Sheehan C, May L, Henkin J, Lobe C, Nagy A, Kerbel RS, et al. (2003). Contrasting effects of VEGF gene disruption in embryonic stem cell–derived *versus* oncogene-induced tumors. *EMBO J* **22**, 4091–4102.

[34] Duxbury MS and Whang EE (2004). RNA interference: a practical approach. *J Surg Res* **117**, 339–344.

[35] Dave RS and Pomerantz RJ (2003). RNA interference: on the road to an alternate therapeutic strategy! *Rev Med Virol* **13**, 373–385.

[36] Schiffelers RM, Ansari A, Xu J, Zhou Q, Tang Q, Storm G, Molema G, Lu PY, Scaria PV, and Woodle MC (2004). Cancer siRNA therapy by tumor selective delivery with ligand-targeted sterically stabilized nanoparticle. *Nucleic Acids Res* **32**, e149.

[37] Brummelkamp TR, Bernards R, and Agami R (2002). Stable suppression of tumorigenicity by virus-mediated RNA interference. *Cancer Cell* **2**, 243–247.

[38] Wilda M, Fuchs U, Wössmann W, and Borkhardt A (2002). Killing of leukemic cells with a BCR/ABL fusion gene by RNA interference (RNAi). *Oncogene* **21**, 5716–5724.